The Kinetics of Hydrolytic Polymerization of ϵ-Caprolactam. II. Determination of the Kinetic and Thermodynamic Constants by Least-Squares Curve Fitting

KAZUO TAI, HIROICHI TERANISHI, YOSHIHIRO ARAI, and TAKASHI TAGAWA, *Research and Development Center, Unitika Ltd., Uji, Kyoto, 611 Japan*

Synopsis

The kinetic and thermodynamic constants of the hydrolytic polymerization of ϵ-caprolactam were determined by least-squares curve fitting. The calculations were carried out using observed kinetic data such as concentrations of ϵ-caprolactam ([CL]), endgroup ([EG]), and ϵ-aminocaproic acid ([ACA]) and time derivatives of each concentration (rates) $\partial[CL]/\partial t$, $\partial[EG]/\partial t$, and $\partial[ACA]/\partial t$. The sets of the converged constants are obtained for the initial water concentrations of 0.42, 0.82, and 1.18 mole/kg. An averaged set of the constants applicable for this range of the initial composition was also evaluated. The compatibility between observed and calculated concentration and rate curves was improved by the use of the newly developed sets of the constants. The mechanism of the polycondensation reaction is also discussed, based on the rate and kinetic constants obtained by this work.

INTRODUCTION

In the preceding paper[1] we pointed out that some discrepancies are found between the kinetic data obtained by the experiments and those obtained by the calculations using the kinetic and thermodynamic constants proposed by Reimschuessel and Nagasubramanian.[2,3] In order to simulate precisely the polymerization reaction in an autoclave, a continuous stirred tank reactor, and a tubular reactor, it is necessary to obtain an improved set of the kinetic and thermodynamic constants. Least-squares curve fitting is employed for this purpose. Although Gerdes et al.[4] had first applied least-squares curve fitting to the determination of the rate and equilibrium constants by using limited kinetic data, details of their results were not reported. In the present work, the determination of all kinetic and thermodynamic constants necessary to formulate the rate equations were performed by the least-squares method.

HYDROLYTIC POLYMERIZATION

The hydrolytic polymerization of ϵ-caprolactam (CL) has been studied by various authors.[1-7] The proposed reaction mechanism, the set of the rate equations derived from the mechanism, and the kinetic and thermodynamic constants are summarized in Table I. Here, x, y, z, and w are the concentrations of CL, endgroup (EG), ϵ-aminocaproic acid (ACA), and water, respectively; k_i^j is the rate constant; K_i is the equilibrium constant; A_i^j is the frequency factor;

Journal of Applied Polymer Science, Vol. 25, 77–87 (1980)

0021-8995/80/0025-0077$01.00

TABLE I
Mechanism and Kinetics

Equilibrium Reactions

1. Ring opening: $\underset{x}{CL} + \underset{w_0 - y}{H_2O} \rightleftharpoons \underset{z}{ACA}$

2. Polycondensation: $P_n + P_m \rightleftharpoons P_{n+m} + H_2O$

$$\underset{y}{-NH_2} + \underset{y}{HOCO-} \rightleftharpoons \underset{x_0 - x - y}{-NHCO-} + \underset{w_0 - y}{H_2O}$$

3. Polyaddition: $\underset{x}{CL} + \underset{y}{P_n} \rightleftharpoons \underset{y - z}{P_{n+1}}$

Rate Equations

$$dx/dt = -k_1[x(w_0 - y) - z/K_1] - k_3[xy - (y - z)/K_3] \quad (1)$$

$$dy/dt = k_1[x(w_0 - y) - z/K_1] - k_2[y^2 - (x_0 - x - y)(w_0 - y)/K_2] \quad (2)$$

$$dz/dt = k_1[x(w_0 - y) - z/K_1] - 2k_2[yz - (y - z)(w_0 - y)/K_2] - k_3(xz - z/K_3) \quad (3)$$

Kinetic and Thermodynamic Constants

$$k_i = k_i^0 + k_i^c y \qquad (i = 1, 2, 3) \quad (4)$$

$$k_i^j = A_i^j \exp(-E_i^j/R/T) \qquad (j = 0, c) \quad (5)$$

$$K_i = \exp[(S_i - H_i/T)/R] \quad (6)$$

E_i^j is the activation energy; S_i is the entropy; H_i is the enthalpy; R is the gas constant; t is the time; and T is the temperature; $i = 1$ means ring-opening, $i = 2$ means polycondensation, and $i = 3$ means polyaddition; $j = 0$ means the non-catalytic reaction and $j = c$ means the catalytic reaction.

LEAST-SQUARES CURVE FITTING

Theory of Least-Squares Curve Fitting

The least-squares method[4,8] can be applied to determine a set of the kinetic and thermodynamic constants:

$$\theta^* = (\theta_p) = (A_i^j, E_i^j, S_i, H_i/j = 0, c; i = 1, 2, 3) \quad (7)^*$$

so that agreement is obtained between observed kinetic data (i.e., a set of tabulated functions of the concentrations and the rates)

$$\nu^{obsd^*} = (\nu_q)^{obsd} = [x(t, T), y(t, T), z(t, T), \partial x(t, T)/\partial t, \partial y(t, T)/\partial t, \partial z(t, T)/\partial t/t = t_1, \ldots, t_m; T = T_1, \ldots, T_n]^{obsd} \quad (8)$$

and the calculated data

$$\nu^{calcd^*} = (\nu_q)^{calcd} = [x(t, T), \ldots]^{calcd} \quad (9)$$

* Eqs. (1)–(6) appear in Table I.

as obtained by numerical solution of the rate equations given in Table I. Here, the asterisk (*) means transpose. Let $\nu_{\mathrm{I}}^{\mathrm{calcd}}$ be the calculated kinetic data corresponding to an initial set of the constants θ_{I}, the differences between observed and calculated data can be given as follows:

$$\Delta\nu_{\mathrm{I}} = \nu^{\mathrm{obsd}} - \nu_{\mathrm{I}}^{\mathrm{calcd}} \tag{10}$$

Using eq. (10), the correction $\Delta\theta_{\mathrm{I}}$ of θ_{I} is evaluated by the following procedure. Let $\nu_{\mathrm{II}}^{\mathrm{calcd}}$ be the calculated data owing to the corrected set of the constants

$$\theta_{\mathrm{II}} = \theta_{\mathrm{I}} + \Delta\theta_{\mathrm{I}} \tag{11}$$

$\Delta\theta_{\mathrm{I}}$ is determined so that the sum of squares of the differences

$$\Psi = (\nu^{\mathrm{obsd}} - \nu_{\mathrm{II}}^{\mathrm{calcd}})^{*}\mathbf{\Lambda}(\nu^{\mathrm{obsd}} - \nu_{\mathrm{II}}^{\mathrm{calcd}}) \tag{12}$$

has its minimum. Here, $\mathbf{\Lambda}$ is the weight matrix. Suppose that ν^{calcd} varies linearly; when θ is moved slightly at its neighborhood, the following expression

$$\nu_{\mathrm{II}}^{\mathrm{calcd}} = \nu_{\mathrm{I}}^{\mathrm{calcd}} + \mathbf{J}_{\mathrm{I}}\Delta\theta_{\mathrm{I}} \tag{13}$$

can be given, where $\mathbf{J}$ is the Jacobian matrix. The introduction of eqs. (10) and (13) into eq. (12) yields the following equation:

$$\Psi = (\Delta\nu_{\mathrm{I}}^{*} - \Delta\theta_{\mathrm{I}}^{*}\mathbf{J}_{\mathrm{I}}^{*})\mathbf{\Lambda}(\Delta\nu_{\mathrm{I}} - \mathbf{J}_{\mathrm{I}}\Delta\theta_{\mathrm{I}}) \tag{14}$$

In order to minimize the sum of squares Ψ, eq. (14) is differentiated with respect to $\Delta\theta_{\mathrm{I}}$ to give the normal equation

$$\mathbf{J}_{\mathrm{I}}^{*}\mathbf{\Lambda}\mathbf{J}_{\mathrm{I}}\Delta\theta_{\mathrm{I}} = \mathbf{J}_{\mathrm{I}}^{*}\mathbf{\Lambda}\Delta\nu_{\mathrm{I}} \tag{15}$$

The correction $\Delta\theta_{\mathrm{I}}$ is obtained from the solution of eq. (15), and the estimated set of the constants θ_{II} is given by eq. (11). In the actual calculation, the numerical solution of the normal eq. (15) is sometimes hard, since the order of the kinetic and thermodynamic constants, as visualized in the succeeding section, varies from 10^{0} to 10^{10}. Thus, the set of the constants θ must be expressed by the product of a scale factor $\mathbf{s}$ and a parameter τ:

$$\theta = \mathbf{s}\tau \tag{16}$$

where $\mathbf{s}$ is a diagonal matrix. τ is used as the set of the parameters to be determined, $\mathbf{s}$ being a fixed constant. The substitution of eq. (16) into eq. (15) yields the transformed normal equation

$$\mathbf{\Phi}_{\mathrm{I}}^{*}\mathbf{\Lambda}\mathbf{\Phi}_{\mathrm{I}}\Delta\tau = \mathbf{\Phi}_{\mathrm{I}}^{*}\mathbf{\Lambda}\Delta\nu_{\mathrm{I}} \tag{17}$$

where $\mathbf{\Phi}$ is the transformed Jacobian matrix given as follows:

$$\mathbf{\Phi} = \mathbf{J}\mathbf{s} \tag{18}$$

The Gauss–Newton iteration process was applied for the set of the transformed equations to obtain a convergence of the curve fitting.

Representation of Jacobian and Weight Matrices

Jacobian Matrix. The Jacobian matrix has a following expression:

$$\mathbf{\Phi} = (\Phi_{pq}) = (\partial\nu_q/\partial\tau_p) = \begin{pmatrix} \mathbf{\Phi}(\mathrm{concn}) \\ \mathbf{\Phi}(\mathrm{rate}) \end{pmatrix} \tag{19}$$

which can be divided into two parts—the concentrations and the rates.

The elements of Φ(concn) for τ are approximated by difference quotients:

$$\partial\nu_q/\partial\tau_p = s_{pp}(\partial\nu_q/\partial\theta_p) = s_{pp}(\Delta\nu_q/\Delta\theta_p) \tag{20}$$

With a given θ_p, the set of the rate eqs. (1)–(3) is solved for θ as well as:

$$\tilde{\theta}^* = (\theta_1,\theta_2,\ldots,\theta_{p-1},\ \theta_p + \Delta\theta_p,\ \theta_{p+1},\ldots) \tag{21}$$

The difference $\nu_q(\tilde{\theta}) - \nu_q(\theta)$ gives the value of $\Delta\nu_q$.

The element of Φ(rate) for τ is expressed analytically by partial differentiation of the rate eqs. (1)–(3) with respect to each τ_p:

$$\partial\nu_q/\partial\tau_p = s_{pp}(\partial\nu_q/\partial\theta_p) \tag{22}$$

For an example, let ν_q and θ_p be $(\partial x/\partial t)(t = t_a,\ T = T_b)$ and A_1^0, respectively; the corresponding element is represented as follows:

$$\begin{aligned}\partial\nu_q/\partial\tau_p &= s_{pp}[\partial(\partial x/\partial t)/\partial k_1^0]_{t=t_a}(\partial k_1^0/\partial A_1^0)_{T=T_b} \\ &= -s_{pp}[x(w_0 - y) - (z/K_1)]_{t=t_a}[\exp(-E_1^0/R/T)]_{T=T_b}\end{aligned} \tag{23}$$

Weight Matrix. The Λ matrix is a diagonal matrix, the element of which is expressed by

$$\Lambda_{qq} = \lambda_q/\sum_t (\nu^{\text{obsd}})^2 \tag{24}$$

where λ_q is the weight for the individual observed data of ν_q and has a close relationship with the uncertainty of the experiment. When ν_q is $x(t = t_a,\ T = T_b)$, for example, the Λ_{qq} is given by

$$\Lambda_{qq} = \lambda_q/\sum_t [x(t,\ T = T_b)^{\text{obsd}}]^2 \tag{25}$$

In the actual calculation, the λ_q value was fixed constant in variation of t for simplicity and was set up so that the contribution of each $\Psi[\nu(T)]$ to the Ψ[total] has the same order.

Modification and Restriction of Parameters

Modification of Hartley. The Gauss–Newton iteration process does not necessarily converge. It sometimes happens that a new parameter $\tau + \Delta\tau$ is calculated with $\Psi(\tau + \Delta\tau) > \Psi(\tau)$. If this is the case, on the line through τ and $\tau + \Delta\tau$ a new point $\tau + \rho\Delta\tau$ is determined in such a way that $\Psi(\tau + \rho\Delta\tau) < \Psi(\tau)$. The trial computations of Ψ for $\rho = (1/2)^n$, $n = 0, 1, 2, \ldots$ were performed to find such a point. This method was studied by Hartley[9] and applied to the field of curve fitting by Gerdes et al.[4]

Restriction of Parameter. During the calculation process, values of rate and equilibrium constants which are evaluated by eqs. (4), (5), (6), (11), (16), and (17) can be calculated that are negative. These values of the rate and equilibrium constants have no physical meaning. Thus, the condition that the rate and equilibrium constants must be restricted,

$$k_i^j > 0, \quad K_i > 0 \qquad j = 0, c;\ i = 1, 2, 3 \tag{26}$$

has to be taken into account.[4]

In order to establish a moderate convergence of the Gauss–Newton iteration process, the restriction that the correction $|\Delta\tau|$ of a cycle must be less than $\delta\%$ of the original $|\tau|$ is also taken into consideration, that is,

$$|\Delta\tau| > \delta|\tau|/100 \tag{27}$$

The value of δ ($40 \geqq \delta \geqq 10\%$) was set up considering the Ψ value corresponding to a cycle of the iteration process.

Experimental Data

The experimental data reported in the preceding paper[1] (Figs. 2–5 of ref. 1) were used for the least-squares curve fitting. The polymerization conditions were as follows: Polymerization temperatures are 230, 240, 250, 260, 270, and 280°C; initial concentrations of water are 0.42, 0.82, and 1.18 mole/kg; polymerization times are from 0 to 10 hr. The rate data were evaluated by the numerical differentiation of the concentration data. Both concentration and rate data were smoothed by the smoothing formula.

Numerical Calculation

The set of rate eqs. (1)–(3) shown in Table I was integrated numerically using the Runge–Kutta–Gill integration scheme with variable time increment.[1] The normal eq. (17) consisting of 18 linear equations was solved numerically by the double-precision sweep-out method. The calculations of the Gauss–Newton iteration process were carried out by a HITAC 8250 computer. In the process the discrepancy factor (DF),

$$DF(\%) = 100 \sum_t \left| X(t, T)^{\text{obsd}} - X(t, T)^{\text{calcd}} \right| \Big/ \sum_t \left| X(t, T)^{\text{obsd}} \right| \tag{28}$$

was used as an adjunct for the object function Ψ. Here, X is x, y, z, $\partial x/\partial t$, $\partial y/\partial t$, or $\partial z/\partial t$, and t is 0 to 10 hr with increments of $\frac{1}{4}$ hr. The estimation process converges within about 10 cycles to the least-squares solution. The process was stopped when the Ψ as well as the DF had their minima.

Since the selection of the starting set of the kinetic and thermodynamic constants θ (i.e., τ) is very important for the direction of the convergence, the following calculation process was applied: As first step the set of the constants published by Reimschuessel and Nagasubramanian[2] was used as an initial set (θ_I) for every cases (w_0 = 0.42, 0.82, and 1.18 mole/kg) and obtained the converged θ: $\theta(w_0 = 0.42)$, $\theta(0.82)$, and $\theta(1.18)$, respectively. As second step, $\theta(0.82)$, $\theta(1.18)$, and averaged θ were used as the starting sets for the initial water concentration of 0.42 mole/kg, and so on, for the other cases. Then, several converged sets for each initial water concentration were obtained. As the final step the most probable set of the constants, the component of which were picked up from those of the sets obtained from first and second steps, was selected for each initial water concentration and improved by the iteration process.

RESULTS AND DISCUSSION

Results of Curve Fitting

The results of the least-squares curve fitting for the three initial water concentrations are given in Tables II, III, IV, and V. Sets 1, 2, and 3 listed in Table II are the converged sets of the kinetic and thermodynamic constants for the initial water concentrations of 0.42, 0.82, and 1.18 mole/kg, respectively. Set 4 is the average of sets 2 and 3, and set 0 is that proposed by Reimschuessel and Nagasubramanian.[2] Tables III and IV give the *DF* values defined by eq. (28) together with those obtained by using the Reimschuessel constants.

Although the Reimschuessel constants, as seen from Table III, gave fair agreement between observed and calculated kinetic data for CL and EG concentrations and rather large discrepancies for ACA concentration and the rates, the *DF* value is reduced much more by this work for the concentration curves of CL, EG, and ACA, especially for the last case. The *DF* values for rate curves are also reduced, except $\partial z/\partial t$ at 280°C for the initial water concentrations of

TABLE II
Kinetic and Thermodynamic Constants[a]

	w_0	i	A_i^0	E_i^0	A_i^c	E_i^c	S_i	H_i
		1	1.6940×10^6	2.1040×10^4	4.1060×10^7	1.8753×10^4	-7.8700×10^0	2.1142×10^3
Set 0	—	2	8.6870×10^9	2.2550×10^4	2.3370×10^{10}	2.0674×10^4	9.3000×10^{-1}	-6.1404×10^3
		3	2.6200×10^9	2.1269×10^4	2.3720×10^{10}	2.0400×10^4	-6.9500×10^0	-4.0283×10^3
		1	4.5397×10^5	1.9655×10^4	4.2695×10^7	1.8807×10^4	-7.8863×10^0	1.6657×10^3
Set 1	0.42	2	2.2243×10^{10}	2.3597×10^4	8.4547×10^7	1.6185×10^4	9.1320×10^{-1}	-6.0287×10^3
		3	2.3265×10^9	2.3108×10^4	1.4762×10^{10}	2.0010×10^4	-7.1121×10^0	-4.2042×10^3
		1	7.4725×10^5	2.0037×10^4	4.0726×10^7	1.8748×10^4	-7.8853×10^0	1.8459×10^3
Set 2	0.82	2	1.9228×10^{10}	2.3287×10^4	7.0413×10^9	1.9913×10^4	9.4348×10^{-1}	-5.9615×10^3
		3	2.7272×10^9	2.3003×10^4	1.8462×10^{10}	2.0169×10^4	-6.9636×10^0	-4.0890×10^3
		1	4.5023×10^5	1.9722×10^4	4.5424×10^7	1.8864×10^4	-7.8838×10^0	1.9756×10^3
Set 3	1.18	2	1.8655×10^{10}	2.3255×10^4	1.7186×10^{10}	2.1427×10^4	9.4400×10^{-1}	-5.9301×10^3
		3	2.9844×10^9	2.2686×10^4	1.4292×10^{10}	2.0045×10^4	-6.9278×10^0	-3.9986×10^3
		1	5.9874×10^5	1.9880×10^4	4.3075×10^7	1.8806×10^4	-7.8846×10^0	1.9180×10^3
Set 4	—	2	1.8942×10^{10}	2.3271×10^4	1.2114×10^{10}	2.0670×10^4	9.4374×10^{-1}	-5.9458×10^3
		3	2.8558×10^9	2.2845×10^4	1.6377×10^{10}	2.0107×10^4	-6.9457×10^0	-4.0438×10^3

[a] $i = 1$, ring opening; $i = 2$, polycondensation; $i = 3$, polyaddition. Superscripts 0 and c mean noncatalytic reaction and catalytic reaction, respectively. Units: w_0 in moles/kg, A_i^0 in kg/mole-hr, A_i^c in kg^2/mole^2-hr, E_i^0 and E_i^c in cal/mole, H_i in cal/mole, S_i in e.u.

TABLE III
Discrepancies between Observed and Calculated Kinetic Data[a]

w_0	K.C.	Temp., °C	Discrepancy factor, %					
			Concentrations			Rates		
			x	y	z	$\partial x/\partial t$	$\partial y/\partial t$	$\partial z/\partial t$
		231	4.6	13.7	47.0	26.3	35.5	71.0
		241	5.8	12.5	49.0	32.3	40.1	73.0
	Set 0	250	7.5	10.0	48.6	36.1	39.5	78.1
		260	9.2	13.3	40.8	44.1	52.6	74.4
		270	9.9	12.9	45.1	44.5	43.5	74.8
		280	10.5	12.3	31.6	45.5	45.2	101.0
0.42		231	7.3	9.5	12.5	15.4	22.3	53.1
		241	6.0	7.6	15.5	15.4	19.3	51.7
	Set 1	250	6.7	6.2	17.5	16.1	22.5	55.0
		260	2.9	2.4	21.7	20.4	24.5	58.6
		270	3.5	4.8	17.4	15.3	19.1	65.5
		280	2.8	5.6	25.2	18.4	19.4	65.4
		230	6.4	6.6	30.9	34.8	40.3	49.7
		240	6.9	8.1	30.9	36.4	41.9	57.8
	Set 0	249	7.0	7.5	34.2	34.7	42.8	63.2
		259	5.7	8.5	32.0	32.9	30.4	67.1
		269	6.8	6.5	26.5	40.7	34.9	64.6
		280	7.8	9.3	26.7	22.5	49.9	61.2
0.82		230	4.9	11.3	17.4	24.3	28.5	49.6
		240	4.6	5.4	12.4	23.7	29.7	31.3
	Set 2	249	4.0	4.2	13.2	20.3	26.1	47.0
		259	3.2	1.4	13.2	14.9	17.5	52.9
		269	3.3	3.3	12.3	22.6	30.4	63.5
		280	3.6	2.2	10.5	34.6	33.7	73.7
		231	6.1	11.2	21.2	36.3	45.1	39.9
		241	5.5	10.8	25.0	34.9	43.4	47.4
	Set 0	250	6.1	11.3	15.8	33.5	38.9	43.6
		260	7.4	11.1	31.3	44.3	35.1	56.1
		269	6.2	11.3	32.6	30.1	46.2	58.2
		281	4.6	12.5	26.9	75.3	99.9	85.1
1.18		231	3.4	6.1	11.7	12.9	23.0	23.4
		241	4.9	2.6	7.3	18.9	18.3	26.0
	Set 3	250	4.3	2.0	13.7	11.6	16.1	28.9
		260	4.9	1.9	17.2	18.7	24.5	42.8
		269	4.0	3.1	20.4	40.3	17.0	51.0
		281	3.9	4.8	15.4	35.3	127.2	84.1

[a] w_0 in mole/kg; K.C. means kinetic and thermodynamic constants.

0.82 and 1.18 mole/kg, and $\partial y/\partial t$ at 280°C for the initial water concentration of 1.18 mole/kg. These exceptions can be explained as follows: The corresponding three observed rate curves have an appreciable uncertainty and cannot be compared with the calculations, since the corresponding experimental concentration curves have a steep up–down or down at early stage of the polymerization and the numerical differentiation cannot follow it. From Table IV, it is found that the averaged DF values for the concentration terms decrease 1/2

TABLE IV
Averaged Discrepancies[a]

w_0	K.C.	av 1	av 2	av 3
	Set 0	21.4	53.2	37.3
0.42	Set 1	9.7	32.1	20.9
	Set 4	11.7	37.0	24.4
	Set 0	14.9	44.8	29.8
0.82	Set 2	7.2	34.7	21.0
	Set 4	7.4	30.2	18.8
	Set 0	14.3	49.6	32.0
1.18	Set 3	7.3	34.4	20.9
	Set 4	7.1	40.9	24.0

[a] w_0 in mole/kg; K.C. means kinetic and thermodynamic constants; av 1 is averaged *DF* for concentration, av 2 for rate, av 3 for concentration and rate.

for every initial water concentration and that the overall averaged *DF* values are reduced as small as 21%. The sum of squares Ψ with weight and without weight (weight is unity) are also given in Table V, and it is found that every term of Ψ is reduced sufficiently well.

A schematic representation of the fitting of the concentration and rate curves, as an example, is given in Figures 1 and 2, where the polymerization temperature is 259°C and the initial water concentration is 0.82 mole/kg. The solid lines are the observed curves, the dotted lines the calculated ones (Reimschuessel's set 0), and the broken lines the calculated ones (this work, set 2), respectively. The *DF* values are written in the figures.

Kinetic and Thermodynamic Constants

Since the equilibrium constants K_i, as described in the preceding paper,[1] are defined by equilibrium concentrations rather than activities, the resultant equilibrium constants depend not only on the temperature but also on the initial composition of the reaction mixture (i.e., the initial water concentration w_0). A similar argument is valid for the rate constants k_i defined by $K_i = k_i/k_i'$. Thus, the kinetic and thermodynamic constants A_i^0, E_i^0, A_i^c, E_i^c, H_i, and S_i are also given by the function of the initial water concentration. From Table II and Figure 3, it is found that every constant depends upon the initial water concentration. In comparison with Reimschuessel constants, the activation energy, entropy, and enthalpy of this work undergo only a slight change, while the frequency factor undergoes a rather large change.

TABLE V
Sum of Squares of the Difference[a]

w_0	K.C.	Ψ_C	Ψ_C^{wt}	Ψ_r	Ψ_r^{wt}	Ψ	Ψ^{wt}
0.42	Set 0	35.8	4.72	112.0	6.10	148.0	10.82
	Set 1	12.3	1.79	20.9	1.81	33.3	3.60
0.82	Set 0	23.9	2.76	135.0	4.17	159.0	6.93
	Set 2	5.6	0.84	80.5	2.80	86.1	3.64
1.18	Set 0	19.0	3.13	404.0	5.14	423.0	8.27
	Set 3	3.0	1.06	111.0	1.29	114.0	2.34

[a] w_0 in mole/kg; K.C., Ψ, *C*, *r*, and *wt* mean kinetic and thermodynamic constants, sum of squares, concentration term, rate term, and weight, respectively.

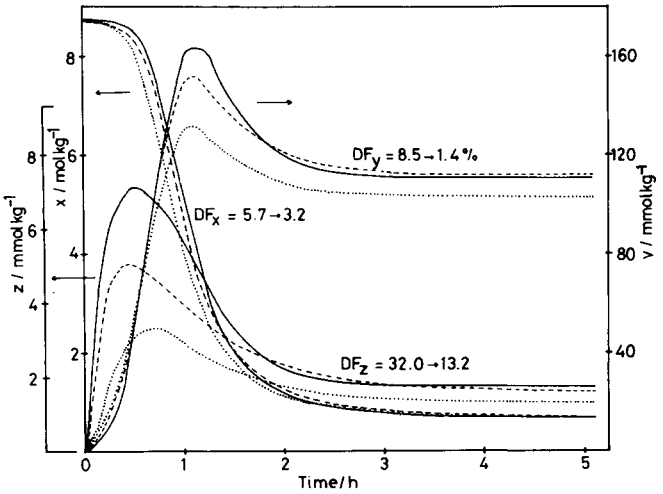

Fig. 1. Comparison of observed and calculated concentration curves of CL, EG, and ACA for initial water concentration of 0.82 mole/kg and temperature of 259°C. Solid lines, dotted lines, and broken lines are the observed, the calculated (Calcd. I) by using Reimschuessel's kinetic and thermodynamic constants, and the calculated (Calcd. II) by this work of set 2, respectively. The *DF* values in the figure are the discrepancy factor defined in the text.

In the course of the actual application of the kinetic and thermodynamic constants, such as for simulation calculations of the polymerization reactions in an autoclave, a continuous stirred tank reactor, a tubular reactor, and a combination of the last two reactors, it is desired to select the constants corresponding to the initial composition of the polymerization mixture. The analytical formulation of the kinetic and thermodynamic constants by a function of the initial water concentration, however, seems to be difficult. Thus, a set of the kinetic and thermodynamic constants such as set 4 in Table II is useful for the limited range of the initial water concentration, as seen from Table IV.

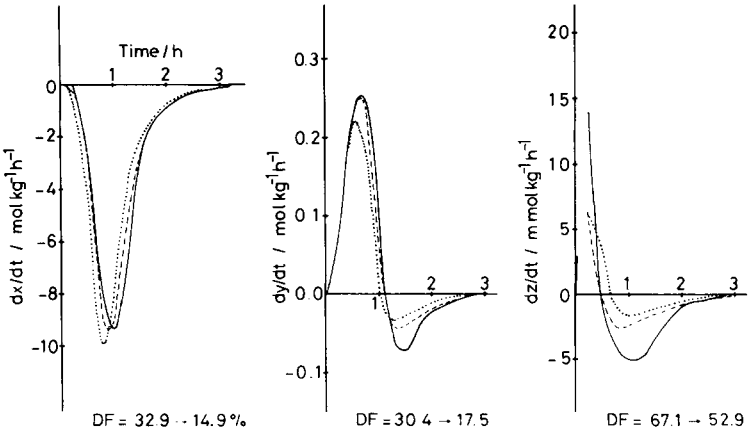

Fig. 2. Comparison of observed and calculated reaction rate curves of CL, EG, and ACA for initial water concentration of 0.82 mole/kg and temperature of 259°C. Solid lines, dotted lines, and broken lines are the observed, the calculated (Calcd. I) by using Reimschuessel's kinetic and thermodynamic constants, and the calculated (Calcd. II) by this work of set 2, respectively. The *DF* values in the figure are the discrepancy factor defined in the text.

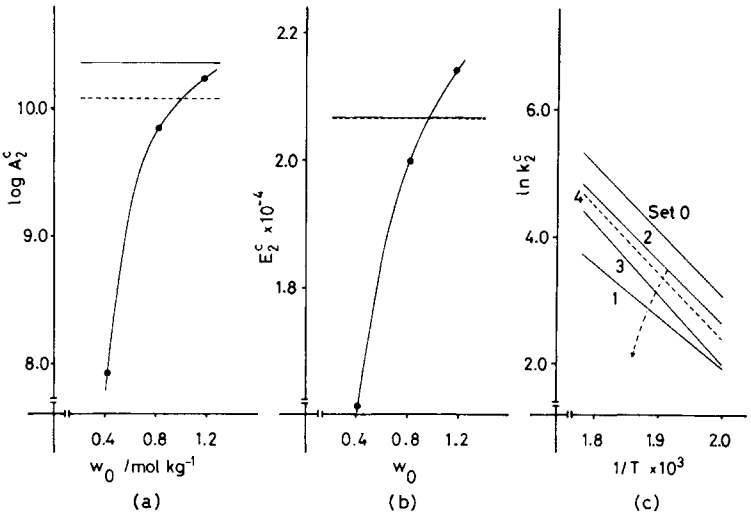

Fig. 3. (a) The converged frequency factor A_2^c of catalytic polycondensation as function of initial water concentration, where solid and broken lines indicate the A_2^c level of set 0 (Reimschuessel's) and set 4, respectively. (b) The converged activation energy E_2^c as function of initial water concentration, where solid and broken lines indicate the E_2^c level of set 0 and set 4. (c) Effect of initial water concentration on the Arrhenius plot (ln k_2^c vs. $1/T$) of catalytic polycondensation. Sets 1, 2, and 3 are the converged sets of the constants for initial water concentrations of 0.42, 0.82, and 1.18 mole/kg, respectively. Set 0 is that of Reimschuessel and Nagasubramanian,[2] and set 4 is the average of sets 2 and 3.

Polycondensation Reaction

Giori and Hayes[10] concluded from a study of the polymerization reactions of some polyamides that the reaction follows a second-order mechanism, i.e., the reaction is not catalyzed by the endgroup. If this is true, the frequency factor A_2^c or the activation energy E_2^c of eq. (5) should have the following limiting values: $A_2^c = 0$ or $E_2^c = \infty$. As seen from Table II and Figure 3, our result, however, does not prove rigorously their conclusion but seems to prove that the reaction is still catalyzed by the endgroup. The decreases of A_2^c and E_2^c, Figures 3(a) and 3(b), and the movement of the Arrhenius plots shown by the arrow in Figure 3(c) with decreasing initial water concentration suggest that the contribution of the catalytic term of the rate constant decreases with decreasing initial water concentration and may be ignored in the range of the initial water concentration investigated by Giori and Hayes.

The authors wish to thank Dr. Akira Tai of Osaka University and Dr. Matsuo Hirami of their laboratory for many helpful discussions and suggestions.

References

1. K. Tai, H. Teranishi, Y. Arai, and T. Tagawa, *J. Appl. Polym. Sci.*, **24**, 211 (1979).
2. H. K. Reimschuessel and K. Nagasubramanian, *Chem. Eng. Sci.*, **27**, 1119 (1972).
3. H. K. Reimschuessel, *J. Polym. Sci. Macromol. Rev.*, **12**, 65 (1977).
4. F. O. Gerdes, P. J. Hoftyzer, J. F. Kemkes, M. Van Loon, and C. Schweigman, *Chem. Eng.*, CE267 (1970).
5. P. H. Hermans, D. Heikens, and P. F. Van Velden, *J. Polym. Sci.*, **30**, 81 (1958).
6. D. Heikens, *J. Polym. Sci.*, **22**, 65 (1956); **35**, 277 (1959).
7. F. Wiloth, *Kolloid Z.*, **143**, 129 (1955); **144**, 58 (1955); *Z. Phys. Chem. Neue Folge*, **11**, 78 (1957).

8. J. Kowalik and M. R. Osborne, *Methods for Unconstrained Optimization Problems*, American Elsevier, New York, 1968.
9. H. O. Hartley, *Technometrics*, **3**, 269 (1961).
10. C. Giori and B. T. Hayes, *J. Polym. Sci. Part A-1*, **8**, 335 (1970).

Received April 27, 1979
Revised August 20, 1979